Infrared spectroscopic study of the low-temperature phase behavior of ammonium sulfate

Tara J. Fortin, John E. Shilling, and Margaret A. Tolbert

Department of Chemistry and Biochemistry and Cooperative Institute for Research in Environmental Sciences, University of Colorado, Boulder, Colorado, USA

Received 26 March 2001; revised 12 November 2001; accepted 18 December 2001; published 22 May 2002.

[1] The low-temperature phase behavior of ammonium sulfate ($(NH_4)_2SO_4$) films has been studied using Fourier transform infrared (FTIR) spectroscopy. While the deliquescence of ammonium sulfate aerosols is well characterized at temperatures above the eutectic of ice and anhydrous ammonium sulfate at 254 K, much less is known about the phase properties at lower temperatures. In the present study, experiments were performed over the temperature range from 166 to 235 K. The apparatus used for this work was a thin-film, high-vacuum apparatus in which the condensed phase is monitored via FTIR spectroscopy and water pressure is monitored with an MKS baratron. Results of experiments performed at low relative humidity (RH) confirm the presence of a ferroelectric phase of ammonium sulfate at temperatures less than 216 ± 8 K. Results of experiments performed as a function of increasing RH demonstrate that a phase transition from crystalline $(NH_4)_2SO_4$ to a metastable aqueous solution (hereafter referred to as deliquescence) occurs at temperatures below the eutectic. Specifically, at temperatures >203 K we observed deliquescence near 88 ± 8% RH. These results are in satisfactory agreement with extrapolated results from experiments performed at temperatures above the eutectic, as well as theory. In experiments performed at temperatures between 166 and 203 K, we sometimes observed deliquescence and sometimes observed direct deposition of ice from the vapor phase, possibly indicating selective heterogeneous nucleation. Ice nucleation prevents the relative humidity from rising to the level needed for deliquescence, thus explaining the variability in our low-temperature results. Possible implications of this work for cirrus cloud formation are also presented. *INDEX TERMS:* 0320 Atmospheric Composition and Structure: Cloud physics and chemistry; 0305 Atmospheric Composition and Structure: Aerosols and particles (0345, 4801); 0365 Atmospheric Composition and Structure: Troposphere—composition and chemistry; 0399 Atmospheric Composition and Structure: General or miscellaneous; *KEYWORDS:* subeutectic, phase changes, cirrus cloud formation, metastability, relative humidity, heterogeneous nucleation

1. Introduction

[2] To understand the role tropospheric aerosols play in the global atmosphere, it is important to know their phase as well as their composition [*Martin*, 2000]. For example, a recent evaluation of upper tropospheric NO_x suggests that as much as 20 to 60% of the NO_x loss rate is attributed to the heterogeneous hydrolysis of N_2O_5 [*Penner et al.*, 1998]. Several laboratory studies have shown that the efficiency of this reaction depends on aerosol phase, with liquid substrates promoting hydrolysis more effectively than solid substrates [*Hanson and Ravishankara*, 1993; *Mozurkewich and Calvert*, 1988]. Furthermore, the initial phase of tropospheric aerosols may be an important factor in the subsequent ice nucleation mechanism. The ice nucleation mechanism ultimately determines the properties of cirrus clouds [e.g., *DeMott et al.*, 1997; *Martin*, 1998; *Tabazadeh and Toon*, 1998], with implications for climate [*DeMott et al.*, 1997; *Jensen and Toon*, 1997; *Liou*, 1986]. The likely phase transitions in atmospheric particles must be characterized as a function of temperature and relative humidity (RH) to help with the prediction of their phase in the upper troposphere [e.g., *Tang and Munkelwitz*, 1993].

[3] Tropospheric sulfate aerosols were once thought to be predominantly composed of H_2SO_4 [e.g., *Sheridan et al.*, 1994]. However, field measurements have revealed that significant amounts of ammonium ions are present [*Talbot et al.*, 1998], indicating that at least some fraction of the sulfate aerosols could exist in neutralized or partially neutralized forms such as ammonium sulfate, ammonium bisulfate, or letovicite. A salt such as ammonium sulfate will remain crystalline when cooled or exposed to increasing water vapor pressure, up to some specific relative humidity known as the deliquescence point [*Seinfeld and Pandis*, 1998]. At this point the salt will readily take up water and form a solution. This transition is thermodynamically driven, with no kinetic inhibition.

[4] The deliquescence behavior of ammonium sulfate has been well studied. Laboratory studies performed at 298 K have demonstrated that ammonium sulfate aerosols deliquesce close to the theoretical value of 80% RH [e.g., *Cohen et al.*, 1987; *Cziczo and Abbatt*, 1999; *Cziczo et al.*, 1997; *Han and Martin*, 1999; *Onasch et al.*, 1999; *Orr et al.*, 1958; *Tang et al.*, 1995; *Tang and Munkelwitz*, 1993, 1994; *Xu et al.*, 1998]. There have been far fewer studies done at temperatures below 298 K [*Cziczo and Abbatt*, 1999; *Onasch et al.*, 1999; *Tang and Munkelwitz*, 1993, 1994; *Xu et al.*, 1998]. These studies have shown behavior similar to the room temperature work, with the deliquescence relative humidity increasing slightly with decreasing temperature. However, until recently [e.g., *Braban et al.*, 2001], these low-temperature deliquescence experiments have been limited to a minimum temperature of approximately 254 K, which corresponds to the eutectic point. In contrast, the temperature range in the upper troposphere is 203–243 K. In order to fully characterize this

0148-0227/02/2001JD000677

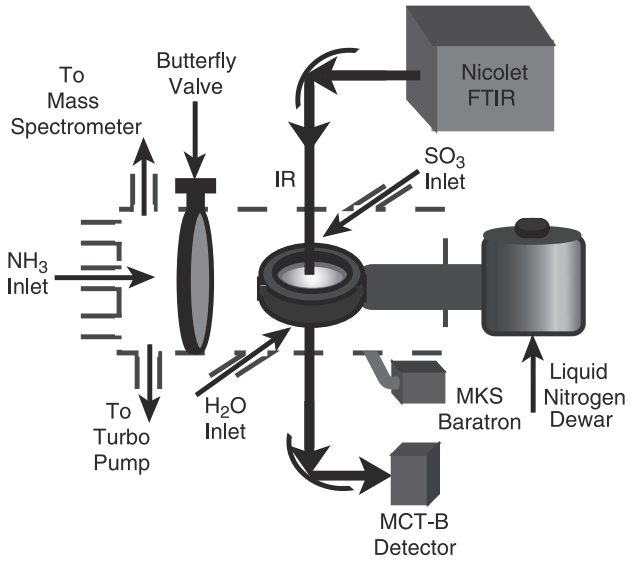

Figure 1. Schematic diagram of the experimental apparatus. The butterfly valve remains open during all experiments in this study.

system and be able to assess its significance in the atmosphere, it is necessary to study the phase behavior at the lower temperature conditions relevant to the upper troposphere.

[5] In this study, we report on the phase behavior of solid ammonium sulfate at temperatures below the eutectic point. First, we probe the low-temperature ferroelectric phase transition. While the presence of the ferroelectric phase is well established [e.g., *Matthias and Remeika*, 1956], it is unclear whether its presence will affect phase behavior as a function of RH. We therefore perform isothermal experiments on both phases where the RH is increased incrementally while we probe for deliquescence and/or ice nucleation using Fourier transform infrared (FTIR) spectroscopy.

2. Experiment

2.1. Thin-Film Apparatus

[6] Experiments were performed using a thin-film, high-vacuum apparatus that has previously been described in detail [*Iraci et al.*, 1995, 1998] and is shown schematically in Figure 1. Briefly, a silicon wafer (2 inch diameter, 0.3 mm thick) is supported in a copper mount that is in thermal contact with a liquid nitrogen reservoir. A desired film temperature is achieved by heating with an annular resistive Kapton heater that is laminated directly to the underside of the silicon wafer and is controlled with a Eurotherm temperature controller. The temperature is measured with T-type thermocouples located at several locations on the mount, including two thermocouples that are fastened in 1-mm holes in the silicon wafer with the aid of thermally conductive silicon paste. Thermocouples are monitored with a PC utilizing LabView data collection software. The two thermocouples attached to the silicon wafer are usually calibrated daily via reference to the ice frost point. However, difficulties were encountered with this procedure. As a result, the temperature measurement is the largest source of error in this study. A detailed discussion of this point will be given later in the paper. The vapors over separate reservoirs of liquid H_2O, liquid NH_3, and solid SO_3 are introduced into the chamber through separate leak valves as needed. To facilitate the achievement of high pressures of water, the H_2O reservoir, as well as the glass manifold line and the leak valve, are heated during experiments. Condensed-phase species are monitored with a Nicolet 740 FTIR spectrometer. For each experiment the spectral resolution is 8 cm^{-1}, and spectra are collected approximately every 5 s. Water pressure is measured with an MKS Baratron gauge that is monitored with the same PC used for the thermocouples. A calibrated UTI 100C quadrupole mass spectrometer is used to verify that H_2O is the only gas-phase species present in the chamber, thereby justifying the use of the baratron.

2.2. Ammonium Sulfate Films

[7] Ammonium sulfate films are made in situ. Figure 2 shows spectra taken at various points during the preparation of a film. First, SO_3 is vapor deposited on top of the silicon wafer at 130 K (spectrum A). Next, approximately 1–1.5 μm of ice is deposited on top of the SO_3 (spectrum B). The film is then warmed at 5 K min^{-1} to approximately 215 K to form a liquid sulfuric acid film (spectrum C). Finally, NH_3 is introduced into the chamber at pressures not exceeding ~2 torr. The film is warmed to approximately 298 K to facilitate diffusion of NH_3 throughout the film and neutralization. Complete neutralization is achieved after 1–2 hours (spectrum D). The film shown in spectrum D compares very well to published spectra for dry ammonium sulfate [*Cziczo et al.*, 1997; *Onasch et al.*, 1999; *Weis and Ewing*, 1996], including those of aerosols. The film is then pumped on overnight in the chamber at a base pressure of 10^{-7} torr to ensure dry conditions at the start of an experiment the next day. Generally, a given film is used for 2 to 3 days, after which the chamber is vented, and the silicon wafer is cleaned off.

2.3. Procedure

[8] Two different types of film experiments were performed during this study. First, ammonium sulfate is known to undergo a ferroelectric phase transition at approximately 223 K [e.g., *Matthias and Remeika*, 1956], whereupon the electron spins become aligned. This change in spin direction is indicated, for example, by a large shift in the dielectric constant of the crystal [*Kamiyoshi*, 1957]. Experiments were performed to verify this transition. In these experiments, no water vapor was introduced into the cham-

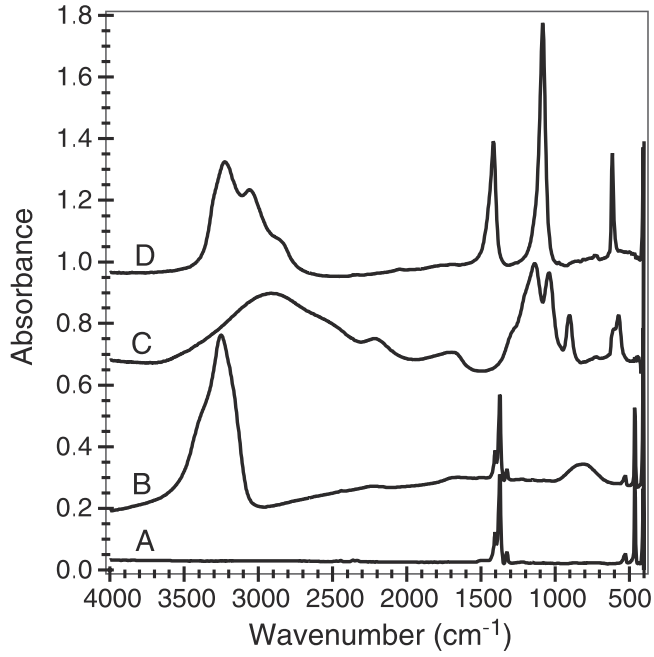

Figure 2. Making an ammonium sulfate film. SO_3 is vapor deposited at 130 K (spectrum A). Ice is then deposited on top of the SO_3 (spectrum B). The film is then warmed at 5 K min^{-1} to ~215 K to form a liquid H_2SO_4 film (spectrum C). Finally, the film is exposed to high pressures of NH_3 for several hours until completely neutralized to give an ammonium sulfate film (spectrum D).

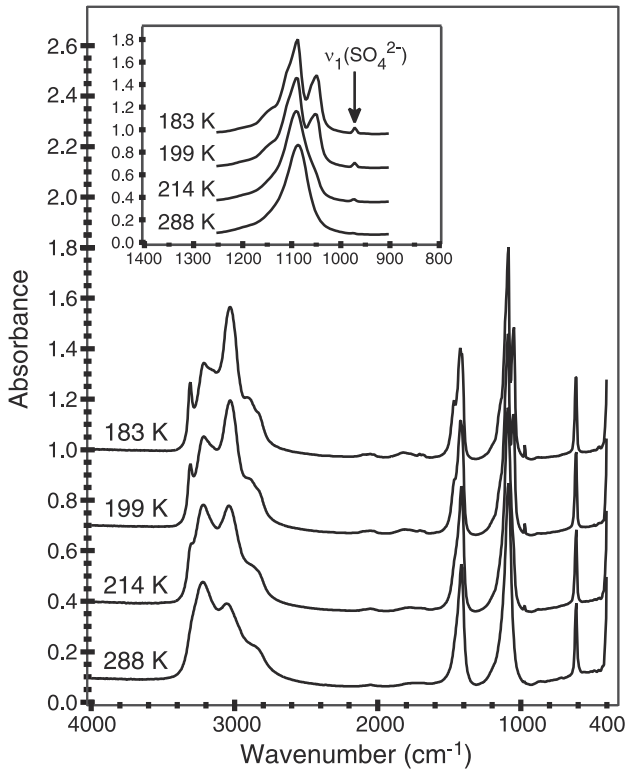

Figure 3. Ferroelectric phase transition in $(NH_4)_2SO_4$. Shown are several IR spectra taken while warming an ammonium sulfate film from 183 to 288 K at a rate of 0.5 K min^{-1}. The spectra have been offset for clarity. Shown in the inset is the spectral region from 900 to 1250 cm^{-1}, expanded to show clearly the changes with temperature. The peak corresponding to the $\nu_1(SO_4^{2-})$ mode is labeled. The sudden appearance of this peak indicates the transition between the paraelectric and ferroelectric phases, occurring at 214 K.

ber. Rather, the temperature was slowly changed while the crystalline film was monitored for changes indicating the ferroelectric phase. Experiments were performed in which the temperature was increased, as well as decreased, to investigate whether the transition was completely reversible.

[9] For all other experiments the temperature was set and allowed to stabilize. Water vapor was then introduced into the chamber. The water pressure was increased incrementally while the film was monitored with FTIR spectroscopy for signs of condensed-phase water. Liquid water is indicated by absorption bands at 3380, 1650, and 650 cm^{-1}, which correspond to the OH stretch, the HOH bend, and the hydrogen bond, respectively. These same bands change in position and sharpen for water ice [*Clapp et al.*, 1995; *Downing and Williams*, 1975]. Specifically, the OH stretch shifts to lower wave numbers, the HOH bend broadens and decreases in intensity, and the hydrogen bond mode narrows, decreases in intensity, and shifts to higher wave numbers. Using these spectral differences, it is possible to distinguish between the formation of aqueous ammonium sulfate and ice nucleation.

3. Results and Discussion

3.1. Ferroelectric Phase Change

[10] It has long been known that ammonium sulfate undergoes a phase transition at 223 K [*Hettner and Simon*, 1928], but it was not until 1956 that it was shown to become ferroelectric below this transition temperature [*Matthias and Remeika*, 1956]. However, ammonium sulfate exhibits behavior uncommon to most known ferroelectric substances. For example, it has a small Curie-Weiss constant [*Onodera et al.*, 1985], and its spontaneous polarization exhibits a peculiar temperature dependence [*Sawada et al.*, 1975; *Unruh*, 1970]. As a result, ammonium sulfate has been classified as an improper ferroelectric [*Kobayashi et al.*, 1972] or a pseudo-proper ferroelectric [*Petzelt et al.*, 1974]. While this ferroelectric phase change is commonly believed to be first order [*Hoshino et al.*, 1958; *O'Reilly and Tsang*, 1967a, 1967b], the specific transition mechanism is not yet well understood. Proposed mechanisms include reorientation of NH_4^+ ions [*O'Reilly and Tsang*, 1967a, 1967b, 1969; *Petzelt et al.*, 1974], molecular distortions of SO_4^{2-} ions [*Jain and Bist*, 1974; *Jain et al.*, 1973], and reorientation of the whole group NH_4^+(I)-SO_4^{2-}-NH_4^+(II), where NH_4^+(I) and NH_4^+(II) refer to the two nonequivalent ammonium ions of the unit cell [*De Sousa Meneses et al.*, 1995].

[11] Several experiments were performed to determine the ferroelectric transition point of our polycrystalline $(NH_4)_2SO_4$ films. As was described in the preceding section, these experiments were performed in the absence of water vapor. The ammonium sulfate film was monitored via FTIR spectroscopy while the temperature was slowly raised or lowered. Figure 3 shows several spectra taken during the course of one of these experiments, where the temperature was increased from 183 to 288 K at a rate of 0.5 K min^{-1}. The spectral region from 900 to 1250 cm^{-1} has been expanded and is shown in the inset. This region corresponds to the $\nu_4(SO_4^{2-})$ mode at approximately 1050 to 1150 cm^{-1} and the $\nu_1(SO_4^{2-})$ mode at approximately 952 to 982 cm^{-1} [*Jain et al.*, 1973; *Weis and Ewing*, 1996]. For the experiment shown in Figure 3 the transition between the paraelectric and the ferroelectric phases occurs at 214 K. The transition is indicated by the distinct spectral features of the two phases. It should be noted that the features described below are in excellent agreement with the IR spectra obtained during the ferroelectric transition in the aerosol experiments of *Chelf and Martin* [2001].

[12] While the experiment shown in Figure 3 was performed by slowly warming the film, converting from the ferroelectric to the paraelectric phase, the following discussion of the changes in spectral features reverses the direction for simplicity. In the paraelectric phase (288 K) the $\nu_3(NH_4^+)$ mode consists of three overlapping diffuse features and a shoulder with peak centers at approximately 2850, 3062, 3219, and 3300 cm^{-1} [*Weis and Ewing*, 1996]. In contrast, in the ferroelectric phase ($\leq$214 K) the shoulder at 3300 cm^{-1} begins growing in, and the relative heights of the peaks at 3219 and 3062 cm^{-1} begin to dramatically change. Additionally, in the $\nu_4(SO_4^{2-})$ region a shoulder begins to appear, eventually splitting to give two peaks where a singlet had existed at room temperature. Finally, in the $\nu_1(SO_4^{2-})$ region a peak becomes visible at approximately 972 cm^{-1}. It is this peak that was used to ultimately determine the transition point.

[13] The symmetric stretch of $SO_4^{2-}(\nu_1)$ is particularly thermosensitive [*Herzberg*, 1945]. This mode is forbidden in IR absorption for perfect tetrahedral symmetry. Therefore its intensity demonstrates the degree of distortion associated with the ion [*Jain and Bist*, 1974; *Jain et al.*, 1973]. Figure 4 shows the temperature-dependent behavior of $\nu_1(SO_4^{2-})$. Specifically, the integrated intensity for 952–982 cm^{-1} is plotted as a function of temperature. At room temperature this band is very weak, as demonstrated in both Figures 3 and 4. However, an abnormal enhancement is observed in the integrated intensity upon transition to the ferroelectric phase. This is associated with a sudden increase in the distortion of the sulfate ion. Following the example of *Jain et al.* [1973], the inflection point of the curve shown in Figure 4 is taken as the ferroelectric transition point (T_t). For the experiment shown in Figure 4 the transition occurs at 214 K.

[14] Subsequent experiments demonstrated similar behavior, with transition points of 213 and 216 K. The transition is

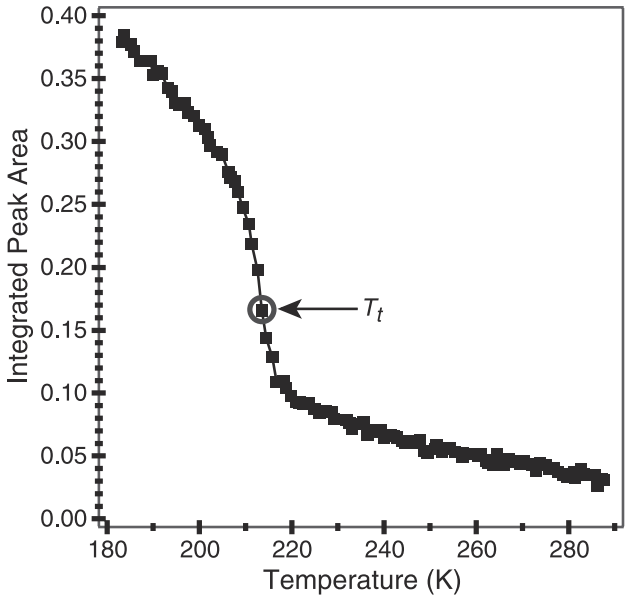

Figure 4. Temperature-dependent behavior of $\nu_1(SO_4^{2-})$. Shown is the integrated intensity for 952–982 cm^{-1} plotted as a function of temperature. T_t denotes the transition point between the paraelectric and ferroelectric phases.

independent of direction and rate of temperature change. As discussed below, the estimated temperature error for these three experiments is ±8 K. Therefore, within our experimental error, our $(NH_4)_2SO_4$ films undergo a reversible, ferroelectric phase transition at temperatures consistent with the 223 K transition point reported in the literature. With this information we were able identify which phase was present for any subsequent experiments. In this way, we could look for possible differences in the low-temperature phase behavior of the paraelectric and ferroelectric phases when the films were exposed to water vapor.

3.2. Deliquescence

[15] Figure 5 shows the phase diagram for ammonium sulfate and water, expressed in terms of temperature and composition. The solid-liquid coexistence lines for $(NH_4)_2SO_4$ and ice were constructed from *Tang and Munkelwitz* [1993] and *Clegg et al.* [1995], respectively. The intersection of these two lines corresponds to the eutectic of ice and anhydrous ammonium sulfate at 254 K (indicated by dashed line in Figure 5). At this point all three phases (aqueous $(NH_4)_2SO_4$, crystalline $(NH_4)_2SO_4$, and ice) are in equilibrium. It is important to note that the phase diagram in Figure 5 is for the $(NH_4)_2SO_4$-H_2O system under conditions of thermodynamic equilibrium. This diagram shows that under those conditions the liquid phase cannot exist below the eutectic. However, metastable solutions of H_2O and H_2SO_4, for example, are regularly observed in both the laboratory [e.g., *Carleton et al.*, 1997] and the atmosphere [e.g., *Sassen and Dodd*, 1988]. The specific question of whether or not it is possible for a salt such as ammonium sulfate to undergo a phase transition from an anhydrous solid to a metastable solution has been a point of contention, with both sides represented in the literature [e.g., *Imre et al.*, 1997; *Martin*, 1998; *Tabazadeh and Toon*, 1998].

[16] In an effort to address this question, several experiments were performed to probe the phase behavior of $(NH_4)_2SO_4$ films upon exposure to increasing relative humidity at temperatures below the eutectic. During a number of these a transition from anhydrous to aqueous ammonium sulfate was observed. Although, strictly speaking, deliquescence refers to a solid to liquid phase transition under conditions of thermodynamic equilibrium, this observed transition from solid to metastable liquid will hereafter be referred to as deliquescence, as has been done by others [e.g., *Braban et al.*, 2001; *Koop et al.*, 2000]. Figure 6a shows one such deliquescence experiment, performed at ~219 K. Several IR spectra taken during the course of the experiment are shown. Spectrum A corresponds to the start of the experiment, with subsequent spectra labeled accordingly. It should be noted that at this temperature the ferroelectric phase should be present and, indeed, spectrum A exhibits the same features indicative of the ferroelectric phase as discussed in the preceding section.

[17] As the relative humidity is increased, no significant changes are observed (spectrum B). However, upon reaching the deliquescence point, spectral features indicative of liquid water become apparent (spectra C–E). Absorption bands at 3380 and 650 cm^{-1} begin to grow in (spectrum C). These bands correspond to the OH stretch and hydrogen bonding in liquid water, respectively. After approximately 1 min, these two features have become more obvious (spectrum E). In addition, a third feature at 1650 cm^{-1}, corresponding to the HOH bend, has grown in by this point.

[18] Spectral changes such as these are more easily seen in the spectral subtractions, shown in Figure 6b. Here, spectrum A has been subtracted out of each subsequent spectrum, and is therefore not shown. These results verify the above observations. Specifically, the subtraction result for spectrum B shows no significant changes occurring up to that point in the experiment. In contrast, spectrum C, taken approximately 5 s later, shows the onset of the same liquid water features discussed above. Subsequent spectra (D–E) show continued growth of these features.

[19] The results shown in Figure 6 demonstrate the feasibility of using FTIR to determine the onset of deliquescence, a point that has also been shown in previous aerosol studies performed at warmer temperatures [*Cziczo and Abbatt*, 1999; *Cziczo et al.*, 1997; *Onasch et al.*, 1999]. Temperature and water pressure measurements are then used to calculate the deliquescence relative humidity (DRH). While our pressure measurement is accurate to ±5%, we had difficulty calibrating our temperature measurement. The presence of the $(NH_4)_2SO_4$ film complicated our usual frost point calibration method. The film tended to deliquesce during the

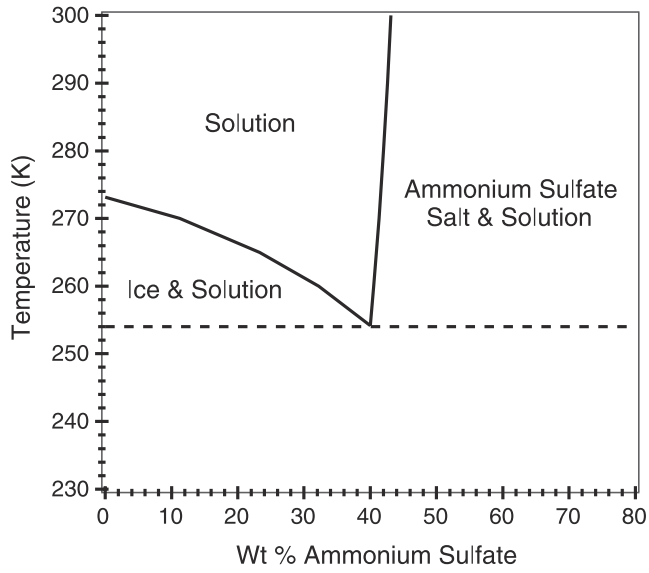

Figure 5. Equilibrium phase diagram for ammonium sulfate and water, plotted as temperature versus composition. Solid lines represent the solid-liquid coexistence lines for ammonium sulfate [*Tang and Munkelwitz*, 1993] and ice [*Clegg et al.*, 1995]. The dashed line marks the anhydrous $(NH_4)_2SO_4$-ice eutectic temperature at 254 K.

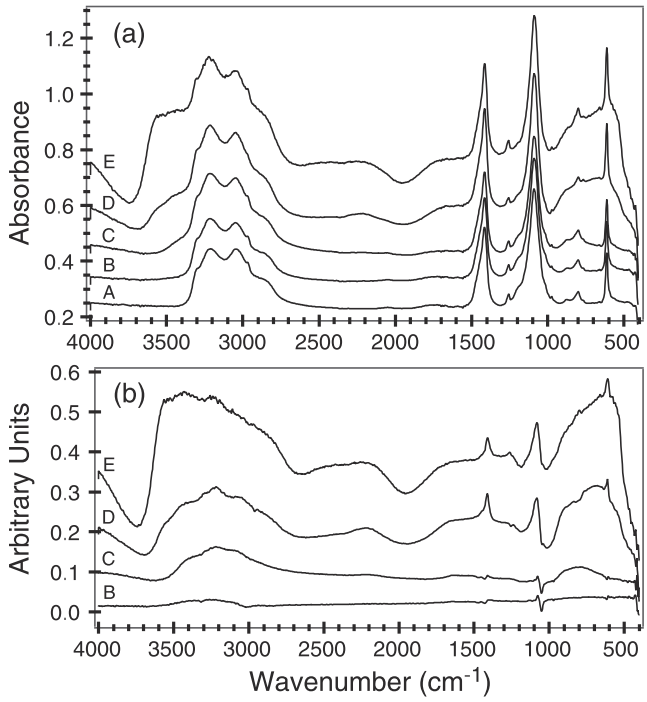

Figure 6. Spectral results for a deliquescence experiment at ~219 K. (a) Selected IR spectra. (b) Results after spectrum A has been subtracted out of each subsequent spectrum. In both panels the spectra have been offset for clarity. Spectrum A is the initial dry ammonium sulfate film. At this temperature the ferroelectric phase is present. Spectrum C is the first spectrum to show signs of water uptake. Subsequent spectra (D–E) show the growth of liquid water features as the film deliquesces.

calibration, resulting in our not being able to perform daily frost point calibrations. Furthermore, day-to-day variability in the thermocouples' behavior precluded the use of some predetermined correction. Instead, we used the spectra themselves to ultimately determine the true temperature, and thus percent RH, in the following manner.

[20] First, spectral subtractions, such as those in Figure 6b, were performed on all the available liquid spectra for a given experiment. Next, peak integrations were performed using both the original spectra and the subtraction results. Specifically, the original spectra were used to integrate the sulfate region from 1025 to 1180 cm^{-1}, while the subtraction results were used to integrate the water region from 1549 to 1751 cm^{-1}. These spectral regions are the same regions used by *Chelf and Martin* [2001] to construct the calibration curve that we used to determine the composition of our liquid films. The expression for this calibration curve is [*Chelf and Martin*, 2001]:

$$\frac{\text{area}(1549-1751\text{cm}^{-1})}{\text{area}(1025-1180\text{cm}^{-1})} = 0.112 + 1.49\exp(-34.9x) + 7.07\exp(-181x), \quad (1)$$

where x is the mole fraction of $(NH_4)_2SO_4$. Once we had determined the composition of our film, we then used that information as input for the thermodynamic model of *Clegg et al.* [1998] to determine the corresponding percent RH. Finally, using the resulting percent RH and the water pressure measured during the experiment, we calculated what the temperature would have to be under those conditions (T_{true}). Comparison to the measured temperature (T_{exp}) allowed us to determine the correction we needed to apply to that particular data set. This procedure was followed for each experiment in which deliquescence was observed.

[21] For example, Figure 7 shows the results of this analysis for the experiment shown in Figure 6. The results are shown as a plot of temperature correction versus time, where the temperature correction is defined as $T_{true} - T_{exp}$. The average correction for this data set was -11.6 ± 1 K. While the correction for any given data set was uniform (see Figure 7), the experiment-to-experiment corrections obtained in this manner ranged from approximately -5 to -20 K, with a median correction of -12 K. These corrections are consistent with those determined by reference to the ice frost point in previous studies performed with the same experimental apparatus.

[22] Corrected temperatures (T_{corr}) and water pressure measurements (P_{exp}, torr) were then used to calculate RH for the entire experiment using

$$\text{RH} = \frac{P_{\text{exp}}(T_{\text{corr}})}{P_{\text{sat}}(T_{\text{corr}})}, \quad (2)$$

where P_{sat} is the saturation vapor pressure with respect to liquid water. P_{sat} is calculated using the *Goff and Gratch* [1946] expression

$$\log e_w = -7.90298\left(\frac{373.16}{T}-1\right) + 5.02808\log\left(\frac{373.16}{T}\right) - 1.3816\times10^{-7}\left(10^{11.344\left(1-\frac{T}{373.16}\right)}-1\right) + 8.1328\times10^{-3}\left(10^{-3.49149\left(\frac{373.16}{T}-1\right)}-1\right) + 3.00571, \quad (3)$$

where e_w is the saturation vapor pressure over a plane surface of liquid water (mbar) and T is the temperature (K). Converting e_w from mbar to torr yields P_{sat}. The error in RH was determined by

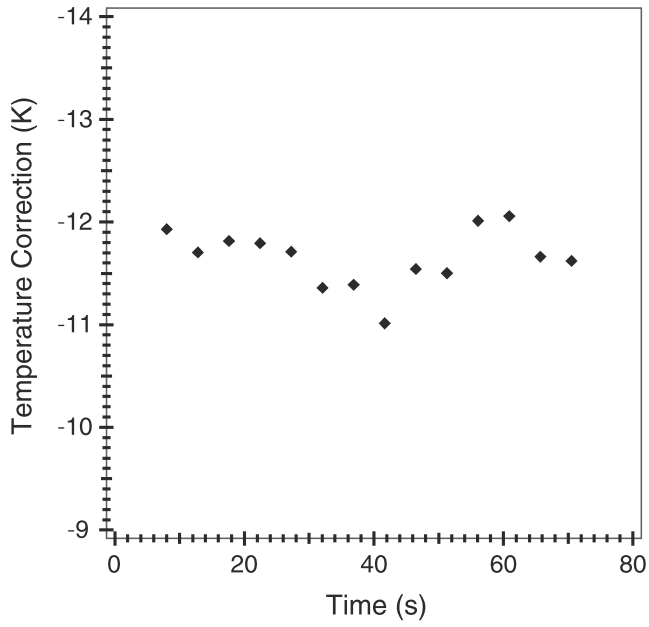

Figure 7. Temperature correction for a typical deliquescence experiment. The temperature correction is shown for all liquid spectra, plotted as a function of time. The temperature correction is defined as the calculated "true" temperature (T_{true}) minus the experimental temperature (T_{exp}). The average correction for this experiment is -11.6 K.

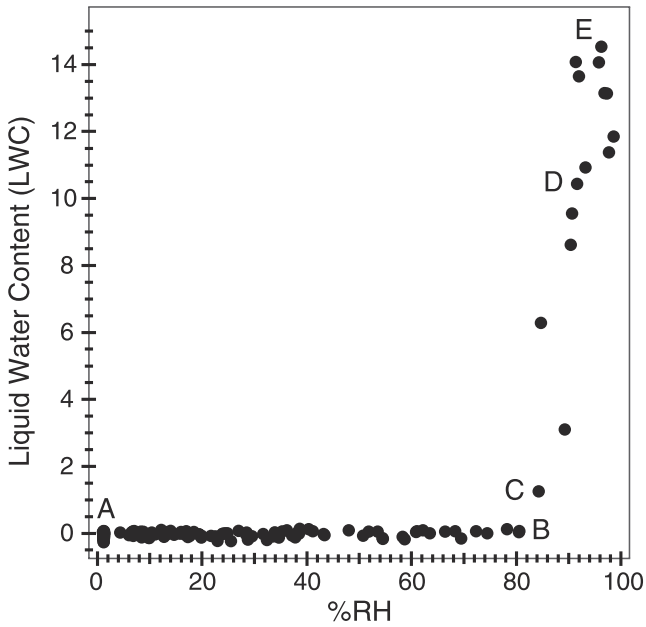

Figure 8. Liquid water content (LWC) of an ammonium sulfate film as a function of relative humidity for a deliquescence experiment at ~219 K. LWC was determined by integrating the water peak at 1549 to 1751 cm^{-1}. Labeled points correspond to labels in Figure 6. The deliquescence relative humidity (DRH) for this experiment is 93 ± 13%.

propagating the errors in P_{exp} and P_{sat}. As was stated earlier, the estimated error in P_{exp} is ±5%. The estimated error in P_{sat} is ±13%. This number corresponds to the error in P_{sat} resulting from a ±1 K error in temperature. We feel that a ±1 K error in temperature is a reasonable estimate since the spread in our calculated corrections, such as those shown in Figure 7, is consistently within ±1 K for a given experiment. The resulting error is ±14% of the experimental RH, with the caveat that the error in the positive direction is reassessed as necessary to ensure that DRH never exceeds 100%.

[23] Unfortunately, for experiments where no liquid spectra were available this method of determining RH could not be used. For those experiments either the overall median temperature correction or the median correction for a given day was used instead. Specifically, for experiments performed on days where no deliquescence was observed, the overall median correction was used. In contrast, on days when deliquescence was observed, the median correction for that particular day was used. For example, for the experiment shown in Figure 3, the temperature correction used was the overall median of −12 K. This correction was used for each of the ferroelectric phase change experiments. Finally, the spread in corrections, either overall or daily, was used as an estimate of the temperature error. This results in an error of ±8 K for the phase change experiments and errors ranging from ±1 to ±4 K for the ice nucleation experiments (discussed in the next section).

[24] To determine the DRH, a hydration curve was constructed, plotted as liquid water content (LWC) versus percent RH (Figure 8). LWC was determined by integrating the water peak at 1549 to 1751 cm^{-1} in the spectral subtractions. For comparison, integrations of the water peak at 3358 to 3532 cm^{-1} were also performed. The graphs for the latter integration region are not shown here but give similar results to the former. The labeled points in Figure 8 correspond to the spectra in Figure 6. From A to B the film exists as anhydrous $(NH_4)_2SO_4$. At this point the DRH is reached, and the film absorbs water to form a saturated solution (B–E). For this experiment, DRH = 93 ± 13%. DRH is determined by averaging the points along the vertical portion of the curve (i.e., all points between and including C and E in Figure 8). When deliquescence occurred, the latent heat released caused the film temperature to rapidly increase. Therefore we are unable to maintain our conditions beyond the point of deliquescence. This prevented us from probing the portion of the hydration curve that corresponds to dilution.

[25] Following the above procedure, the DRH was determined for all experiments in which deliquescence was observed. The results are summarized in Figure 9, plotted as percent DRH versus temperature. A theoretical curve derived from the thermodynamic model of *Clegg et al.* [1998] and the ice saturation line are both shown. In addition, a second line is shown. This line was calculated using the equation

$$\ln(\mathrm{DRH}) = a + \frac{b}{T} + \frac{c}{T^2} + \frac{d}{T^3}, \tag{4}$$

where DRH is the deliquescence relative humidity in percent, T is the temperature in kelvins, and the parameters are defined as $a = 4.9058$, $b = -6.1731 \times 10^2$, $c = 2.0627 \times 10^5$, and $d = -2.0521 \times 10^7$ [*Tabazadeh and Toon*, 1998]. Both lines have been extrapolated to include the temperatures covered in this study (166 to 235 K). As was discussed in the introduction, several studies have been performed at temperatures >254 K [e.g., *Cziczo and Abbatt*, 1999; *Onasch et al.*, 1999; *Tang and Munkelwitz*, 1993, 1994; *Xu et al.*, 1998]. The data from these studies are not shown in Figure 9, but they lie along the lines shown.

[26] There are several conclusions to draw from these results. First, there is significant evidence supporting the occurrence of deliquescence below the eutectic point at 254 K. In contrast, *Xu et al.* [1998] report a solid-solid phase transition to form a tetrahydrate phase. However, *Xu et al.* [1998] do report an observation of what is qualitatively described as "partial deliquescence" under

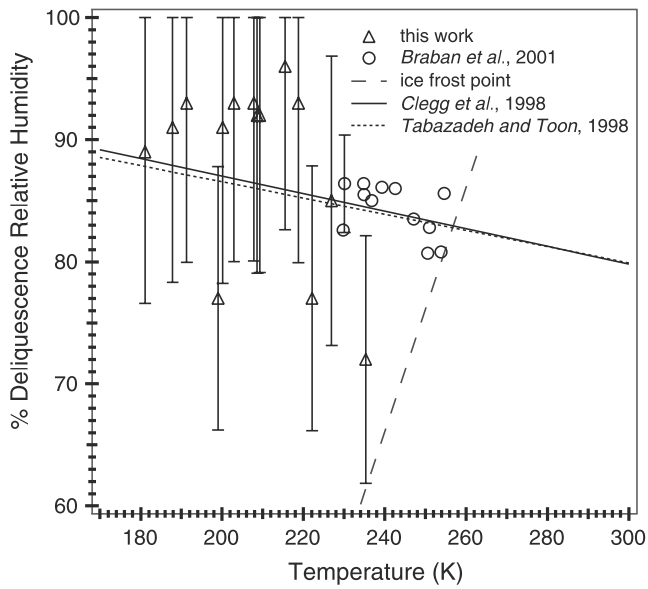

Figure 9. Summary of deliquescence experiments. The open triangles are data from this study. The error bars represent an error equal to 14% of the experimental DRH, adjusted in the positive direction to ensure DRH is not greater than 100%. Temperature error bars are on the order of the symbol size (±1 K), and therefore are not shown. Also included are subeutectic data from the study of *Braban et al.* [2001] (open circles), an extrapolated fit expression [*Tabazadeh and Toon*, 1998] (dotted line), an extrapolated theoretical curve [*Clegg et al.*, 1998] (solid line), and the ice saturation line (dashed line).

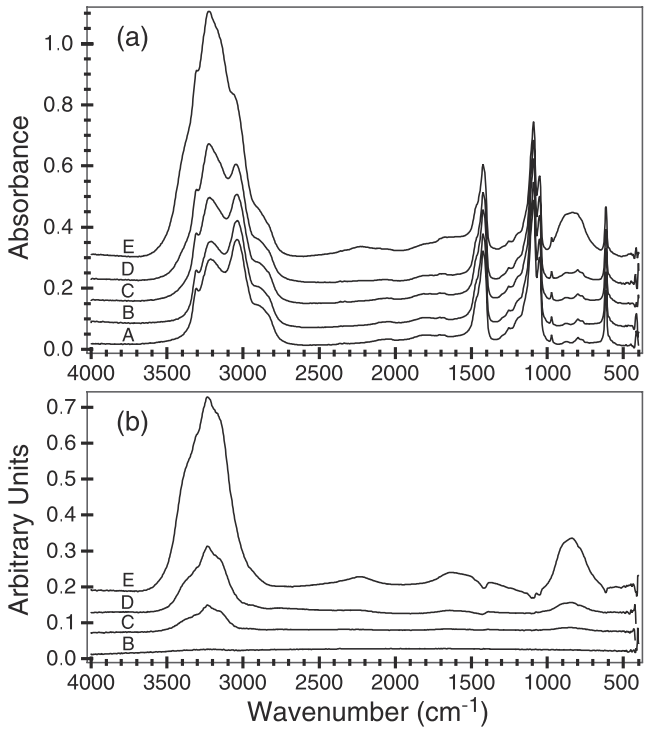

Figure 10. Spectral results for an ice experiment at ~182 K. (a) Selected IR spectra. (b) Results after spectrum A has been subtracted out of each subsequent experiment. In both panels the spectra have been offset for clarity. Spectrum A is the initial dry ammonium sulfate film. At this temperature the ferroelectric phase is present. Spectrum C is the first to show signs of ice nucleation. The ice features increase in intensity as the ice continues to grow (D–E).

nonequilibrium water vapor conditions. Furthermore, our observations are in agreement with a recent study by *Braban et al.* [2001] (see Figure 9). This study reports deliquescence of ammonium sulfate between 229 and 295 K; however, only those results obtained at subeutectic temperatures have been shown for comparison. Second, within experimental error (±14% of the DRH), comparison to the extrapolated fits shows satisfactory agreement with thermodynamically predicted RH values. For example, an extrapolated fit to our data yields a DRH at room temperature that, within our experimental error, agrees with the accepted value of 80%. Finally, deliquescence experiments were performed at temperatures both above and below the ferroelectric phase transition, yet no difference in the behavior of these two phases was observed.

3.3. Ice Nucleation

[27] While deliquescence was observed in approximately half of the experiments we performed, we observed ice formation in the other half. Figure 10a shows the results of one such experiment, performed at 182 ± 1 K. The temperature has been corrected in the manner previously discussed. Specifically, the correction applied to this experiment was −18 K, the median for that particular day. Several IR spectra taken during the course of the experiment are shown. As before, spectrum A corresponds to the start of the experiment, with subsequent spectra labeled accordingly. Again, at this temperature, the ferroelectric phase should be present and, indeed, spectrum A exhibits the features indicative of this phase.

[28] As the relative humidity is increased, no significant changes are observed (spectrum B). However, increasing the water pressure slightly results in the appearance of spectral features indicative of water ice (spectra C–E). Specifically, by spectrum E, absorption bands at 3225, 1650, and 840 cm^{-1} have become obvious. As was discussed earlier, these bands correspond to the OH stretch, the HOH bend, and hydrogen bonding (libration), respectively. Furthermore, these features differ in their appearance from the corresponding features in liquid water. The OH stretch has shifted to lower wave numbers, the HOH bend has broadened and decreased in intensity, and the libration has decreased in intensity and shifted to higher wave numbers.

[29] Again, spectral subtractions were performed and are shown in Figure 10b. Here spectrum A has been subtracted out of each subsequent spectrum, and is therefore not shown. These results verify the above observations. Specifically, the subtraction result for spectrum B shows no significant changes occurring up to that point in the experiment. In contrast, spectrum C shows the onset of the same water ice features discussed above. Subsequent spectra (D–E) show continued growth of these features. Of particular note are the relative heights of the OH stretch and the libration. In Figure 10b the libration peak is approximately half the size of the OH stretch peak. In contrast, in Figure 6b the spectrum for liquid water shows these two peaks to be approximately equal in height. Finally, within our limit of detection, the spectral subtractions show no signs of liquid water prior to ice nucleation. While we cannot rule out the existence of a small amount of deliquescence below our detection limit, we conclude that what we are most likely observing is the direct vapor deposition of ice onto crystalline $(NH_4)_2SO_4$. Recalling that we were unable to determine temperature corrections when ice was observed, we were not able to accurately determine the RH for these experiments. Despite this, as the result of rough estimates of RH, we hypothesize that ice nucleation occurs at relative humidities less than the deliquescence RH. Furthermore, vapor deposition of ice on our silicon substrate is eliminated as a possible explanation since previous experiments have shown that this requires relative humidities greater than 90%. It thus appears that the ice is nucleating on ammonium sulfate via vapor deposition without going through a liquid solution.

[30] Experiments where ice was observed were performed over the temperature range 166–203 K, while deliquescence was observed over the range 181–235 K. One point that becomes immediately clear is that there is a significant degree of overlap in the conditions under which these two distinct results were observed. Efforts were made to explain this overlap through correlation with differences in experimental procedure, such as the rate of change in RH. However, no correlation could be found. Moreover, upon further consideration, the overlap in the data is not completely unexpected when one considers the nature of the ice nucleation process.

[31] Unlike deliquescence, nucleation is kinetically hindered. According to nucleation theory [*Pruppacher and Klett*, 1997] there is an energy barrier associated with the formation of a critical-sized germ. Additionally, ice nucleation is a stochastic process. Therefore it is reasonable to conclude that ice will not always nucleate under a specific set of conditions. We believe this to be the case for the experiments in which we were able to achieve deliquescence. Specifically, for temperatures below 250 K, saturation with respect to ice is achieved at lower water pressures than those required to reach the deliquescence relative humidity. Furthermore, this difference between the saturation vapor pressure of ice and the ammonium sulfate deliquescence RH increases as temperature decreases. Therefore one might expect ice to nucleate first, and for those experiments where we observed ice, this was the case. However, owing to the stochastic nature of the nucleation process, ice will not necessarily nucleate. Consequently, on those occasions where we were able to achieve deliquescence, a critical-sized ice germ was not able to form, thereby allowing us to reach a RH high enough for deliquescence to occur.

[32] These conclusions are supported by additional experiments performed in our laboratory (J. E. Shilling, unpublished data,

2001). Similar to the *Braban et al.* [2001] study, these experiments were performed on ammonium sulfate particles that were atomized and sprayed onto a gold surface, utilizing FTIR spectroscopy to probe phase changes. Isothermal experiments where the particles were exposed to increasing RH were performed from 180 to 240 K. The results show that ice usually nucleates at relative humidities considerably less than the 80–90% required for deliquescence. While deliquescence followed by rapid ice nucleation cannot be definitively ruled out, ice deposition appears to be the most likely nucleation mechanism. Furthermore, the vapor deposition of ice appears to be highly selective, with ice nucleating on just a few select particles, forming small pillars of ice rather than a more uniform film over the entire available surface. It is not clear what is special about the few particles that form ice. It is possible that a particular crystal face or impurity could have been present on those particles. In contrast, in the film experiments there may have been fewer of the "special" nuclei. This would explain why we were able to avoid ice nucleation in at least half of the experiments, thereby allowing us to reach a RH sufficient for deliquescence. However, whenever we were able to reach a high enough RH, deliquescence was always observed. As was stated previously, once deliquescence did occur, we were unable to maintain control over our experimental conditions. At this point we ended our experiments. Therefore we could not observe ice nucleating out of solution.

4. Conclusions

[33] The three main results of this work are as follows. First, ammonium sulfate is observed to deliquesce at temperatures as low as ~181 K. However, in light of the large uncertainties in this study, additional investigations of this metastable phase transition would be advantageous. Second, definitive conclusions regarding the effectiveness of atmospheric $(NH_4)_2SO_4$ as an ice nucleus are difficult to make without further study. Our film results imply that $(NH_4)_2SO_4$ is not the most effective ice nucleus since ice was not observed in every case, despite being saturated with respect to ice. However, the observation of ice on occasion indicates that given the right conditions, $(NH_4)_2SO_4$ could be an effective heterogeneous ice nucleus. This conclusion is supported by additional experiments performed in our laboratory (J. E. Shilling, unpublished data, 2001). Finally, the presence of the ferroelectric phase appears to have no effect on the low-temperature phase behavior of ammonium sulfate.

[34] With respect to the atmosphere, these results may contribute to the discussion of cirrus cloud formation mechanisms. Cirrus clouds are sometimes thought to form via homogeneous freezing of liquid sulfate aerosols [e.g., *DeMott et al.*, 1994; *Heymsfield and Sabin*, 1989; *Sassen and Dodd*, 1988; *Tabazadeh et al.*, 1997]. Alternatively, ice formation via two different heterogeneous pathways is possible. The first involves direct deposition of ice from the vapor phase onto a solid aerosol substrate. It has been suggested that such a mechanism would become less viable at the cold temperatures that exist in the upper troposphere "since the work against surface forces required to create a critical ice germ increases with decreasing temperature" [*Jensen and Toon*, 1997, p. 250]. However, to our knowledge, no laboratory investigations have been performed to rule out the possibility. The second pathway involves solid inclusions, such as soot or crustal material, within liquid aerosols that may initiate the heterogeneous freezing of ice [e.g., *DeMott et al.*, 1997; *Jensen and Toon*, 1997]. As was briefly discussed in the introduction, the ice nucleation mechanism ultimately determines the properties of the cloud [e.g., *DeMott et al.*, 1997]. Therefore it would be advantageous to be able to determine which mechanism dominates and under what conditions.

[35] The results of our film studies suggest that it is possible for $(NH_4)_2SO_4$ to exist as a liquid at the cold temperatures of the upper troposphere. This would be consistent with cirrus cloud formation via homogeneous nucleation. However, the observation of ice on occasion, particularly when interpreted in light of additional experiments currently being performed in our laboratory, seems to indicate that a few special $(NH_4)_2SO_4$ particles could be relatively efficient heterogeneous ice nuclei. Determining exactly how effective these particles are and what specific properties allow for such efficient ice nucleation to occur are points deserving of further investigation.

[36] **Acknowledgments.** We thank J. H. Chelf and S. T. Martin for supplying us with their calibration and J. P. D. Abbatt for communication of results, both prior to publication. Additionally, we thank S. T. Martin, T. B. Onasch, and D. J. Cziczo for helpful discussions. This work was supported by grants from NASA-SASS (SA98-0005) and NSF (ATM-9711969). T.J.F. was supported by a NASA ESS Fellowship (NGT5-301136).

References

Braban, C. F., D. J. Cziczo, and J. P. D. Abbatt, Deliquescence of ammonium sulfate particles at sub-eutectic temperatures, *Geophys. Res. Lett.*, *28*, 3879–3882, 2001.

Carleton, K. L., D. M. Sonnenfroh, W. T. Rawlins, B. E. Wyslouzil, and S. Arnold, Freezing behavior of single sulfuric acid aerosols suspended in a quadrupole trap, *J. Geophys. Res.*, *102*, 6025–6033, 1997.

Chelf, J. H., and S. T. Martin, Homogeneous ice nucleation in aqueous ammonium sulfate aerosol particles, *J. Geophys. Res.*, *106*, 1215–1226, 2001.

Clapp, M. L., R. E. Miller, and D. R. Worsnop, Frequency-dependent optical constants of water ice obtained directly from aerosol extinction spectra, *J. Phys. Chem.*, *99*, 6317–6326, 1995.

Clegg, S. L., S. S. Ho, C. K. Chan, and P. Brimblecombe, Thermodynamic properties of aqueous $(NH_4)_2SO_4$ to high supersaturation as a function of temperature, *J. Chem. Eng. Data*, *40*, 1079–1090, 1995.

Clegg, S. L., P. Brimblecombe, and A. S. Wexler, Thermodynamic model of the system H^+-NH_4^+-SO_4^{2-}-NO_3^--H_2O at tropospheric temperatures, *J. Phys. Chem. A*, *102*, 2137–2154, 1998. (Available at http://www.hpc1.uea.ac.uk/~e770/aim.html)

Cohen, M. D., R. C. Flagan, and J. H. Seinfeld, Studies of concentrated electrolyte solutions using the electrodynamic balance, 1, Water activities for single-electrolyte solutions, *J. Phys. Chem.*, *91*, 4563–4574, 1987.

Cziczo, D. J., and J. P. D. Abbatt, Deliquescence, efflorescence, and supercooling of ammonium sulfate aerosols at low temperature: Implications for cirrus cloud formation and aerosol phase in the atmosphere, *J. Geophys. Res.*, *104*, 13,781–13,790, 1999.

Cziczo, D. J., J. B. Nowak, J. H. Hu, and J. P. D. Abbatt, Infrared spectroscopy of model tropospheric aerosols as a function of relative humidity: Observation of deliquescence and crystallization, *J. Geophys. Res.*, *102*, 18,843–18,850, 1997.

DeMott, P. J., M. P. Meyers, and W. R. Cotton, Parameterization and impact of ice initiation processes relevant to numerical model simulations of cirrus clouds, *J. Atmos. Sci.*, *51*, 77–90, 1994.

DeMott, P. J., D. C. Rogers, and S. M. Kreidenweis, The susceptibility of ice formation in upper tropospheric clouds to insoluble aerosol components, *J. Geophys. Res.*, *102*, 19,575–19,584, 1997.

De Sousa Meneses, D., G. Hauret, P. Simon, F. Bréhat, and B. Wyncke, Phase-transition mechanism in $(NH_4)_2SO_4$, *Phys. Rev. B*, *51*, 2669–2677, 1995.

Downing, H. D., and D. Williams, Optical constants of water in the infrared, *J. Geophys. Res.*, *80*, 1656–1661, 1975.

Goff, J. A., and S. Gratch, Low-pressure properties of water from −160 to 212 F, *Trans. Am. Soc. Heat. Vent. Eng.*, *52*, 95–121, 1946.

Han, J.-H., and S. T. Martin, Heterogeneous nucleation of the efflorescence of $(NH_4)_2SO_4$ particles internally mixed with Al_2O_3, TiO_2, and ZrO_2, *J. Geophys. Res.*, *104*, 3543–3553, 1999.

Hanson, D. R., and A. R. Ravishankara, Reaction of $ClONO_2$ with HCl on NAT, NAD, and frozen sulfuric acid and hydrolysis of N_2O_5 and $ClONO_2$ on frozen sulfuric acid, *J. Geophys. Res.*, *98*, 22,931–22,936, 1993.

Herzberg, G., *Molecular Spectra and Molecular Structure,* vol. 2, *Infrared and Raman Spectra of Polyatomic Molecules*, 632 pp., Van Nostrand Reinhold, New York, 1945.

Hettner, G., and F. Simon, Ultrarotspektren von ammoniumsalzen im umlagerungsgebiet, *Z. Phys. Chem. B*, *1*, 293–300, 1928.

Heymsfield, A. J., and R. M. Sabin, Cirrus crystal nucleation by homogeneous freezing of solution droplets, *J. Atmos. Sci.*, *46*, 2252–2264, 1989.

Hoshino, S., K. Vedam, Y. Okaya, and R. Pepinsky, Dielectric and thermal study of $(NH_4)_2SO_4$ and $(NH_4)_2BeF_4$ transitions, *Phys. Rev.*, *112*, 405–412, 1958.

Imre, D. G., J. Xu, I. N. Tang, and R. McGraw, Ammonium bisulfate/water equilibrium and metastability phase diagrams, *J. Phys. Chem. A*, *101*, 4191–4195, 1997.

Iraci, L. T., A. M. Middlebrook, and M. A. Tolbert, Laboratory studies of the formation of polar stratospheric clouds: Nitric acid condensation on thin sulfuric acid films, *J. Geophys. Res.*, *100*, 20,969–20,977, 1995.

Iraci, L. T., T. J. Fortin, and M. A. Tolbert, Dissolution of sulfuric acid tetrahydrate at low temperatures and subsequent growth of nitric acid trihydrate, *J. Geophys. Res.*, *103*, 8491–8498, 1998.

Jain, Y. S., and H. D. Bist, A point charge model for the ferroelectric transition in ammonium sulphate, *Phys. Status Solidi B*, *62*, 295–300, 1974.

Jain, Y. S., H. D. Bist, and G. C. Upreti, The ferroelectric phase transition in ammonium sulphate, *Chem. Phys. Lett.*, *22*, 572–575, 1973.

Jensen, E. J., and O. B. Toon, The potential impact of soot particles from aircraft exhaust on cirrus clouds, *Geophys. Res. Lett.*, *24*, 249–252, 1997.

Kamiyoshi, K.-I., Effect of electric field on the phase transition of ammonium sulfate, *J. Chem. Phys.*, *26*, 218–219, 1957.

Kobayashi, J., Y. Enomoto, and Y. Sato, A phenomenological theory of dielectric and mechanical properties of improper ferroelectric crystals, *Phys. Status Solidi B*, *50*, 335–343, 1972.

Koop, T., A. Kapilashrami, L. T. Molina, and M. J. Molina, Phase transitions of sea-salt/water mixtures at low temperatures: Implications for ozone chemistry in the polar marine boundary layer, *J. Geophys. Res.*, *105*, 26,393–26,402, 2000.

Liou, K.-N., Influence of cirrus clouds on weather and climate processes: A global perspective, *Mon. Weather Rev.*, *114*, 1167–1199, 1986.

Martin, S. T., Phase transformations of the ternary system $(NH_4)_2SO_4$-H_2SO_4-H_2O and the implications for cirrus cloud formation, *Geophys. Res. Lett.*, *25*, 1657–1660, 1998.

Martin, S. T., Phase transitions of aqueous atmospheric aerosols, *Chem. Rev.*, *100*, 3403–3453, 2000.

Matthias, B. T., and J. P. Remeika, Ferroelectricity in ammonium sulfate, *Phys. Rev.*, *103*, 262, 1956.

Mozurkewich, M., and J. G. Calvert, Reaction probability of N_2O_5 on aqueous aerosols, *J. Geophys. Res.*, *93*, 15,889–15,896, 1988.

Onasch, T. B., R. L. Siefert, S. D. Brooks, A. J. Prenni, B. Murray, M. A. Wilson, and M. A. Tolbert, Infrared spectroscopic study of the deliquescence and efflorescence of ammonium sulfate aerosol as a function of temperature, *J. Geophys. Res.*, *104*, 21,317–21,326, 1999.

Onodera, A., O. Cynshi, and Y. Shiozaki, Landau theory of the ferrielectric phase transition with two order parameters, *J. Phys. C*, *18*, 2831–2841, 1985.

O'Reilly, D. E., and T. Tsang, Deuteron magnetic resonance and proton relaxation times in ferroelectric ammonium sulfate, *J. Chem. Phys.*, *46*, 1291–1300, 1967a.

O'Reilly, D. E., and T. Tsang, First-order ferroelectric transition in $(NH_4)_2SO_4$, *J. Chem. Phys.*, *46*, 1301–1304, 1967b.

O'Reilly, D. E., and T. Tsang, Order-disorder transition in ferroelectric ammonium sulfate, *J. Chem. Phys.*, *50*, 2274–2275, 1969.

Orr, C., Jr., F. K. Hurd, and W. J. Corbett, Aerosol size and relative humidity, *J. Colloid Sci.*, *13*, 472–482, 1958.

Penner, J. E., D. J. Bergmann, J. J. Walton, D. Kinnison, M. J. Prather, D. Rotman, C. Price, K. E. Pickering, and S. L. Baughcum, An evaluation of upper troposphere NO_x with two models, *J. Geophys. Res.*, *103*, 22,097–22,113, 1998.

Petzelt, J., J. Grigas, and I. Mayerová, Far infrared properties of the pseudoproper ferroelectric ammonium sulfate, *Ferroelectrics*, *6*, 225–234, 1974.

Pruppacher, H. R., and J. D. Klett, *Microphysics of Clouds and Precipitation*, 2nd ed., 954 pp., Kluwer Acad., Norwell, Mass., 1997.

Sassen, K., and G. C. Dodd, Homogeneous nucleation rate for highly supercooled cirrus cloud droplets, *J. Atmos. Sci.*, *45*, 1357–1369, 1988.

Sawada, A., S. Ohya, Y. Ishibashi, and Y. Takagi, Ferroelectric phase transition in $(NH_4)_2SO_4$-K_2SO_4 mixed crystals, *J. Phys. Soc. Jpn.*, *38*, 1408–1414, 1975.

Seinfeld, J. H., and S. N. Pandis, *Atmospheric Chemistry and Physics: From Air Pollution to Climate Change*, 1326 pp. , John Wiley, New York, 1998.

Sheridan, P. J., C. A. Brock, and J. C. Wilson, Aerosol particles in the upper troposphere and lower stratosphere: Elemental composition and morphology of individual particles in northern midlatitudes, *Geophys. Res. Lett.*, *21*, 2587–2590, 1994.

Tabazadeh, A., and O. B. Toon, The role of ammoniated aerosols in cirrus cloud nucleation, *Geophys. Res. Lett.*, *25*, 1379–1382, 1998.

Tabazadeh, A., E. J. Jensen, and O. B. Toon, A model description for cirrus cloud nucleation from homogeneous freezing of sulfate aerosols, *J. Geophys. Res.*, *102*, 23,845–23,850, 1997.

Talbot, R. W., J. E. Dibb, and M. B. Loomis, Influence of vertical transport on free tropospheric aerosols over the central USA in springtime, *Geophys. Res. Lett.*, *25*, 1367–1370, 1998.

Tang, I. N., and H. R. Munkelwitz, Composition and temperature dependence of the deliquescence properties of hygroscopic aerosols, *Atmos. Environ., Part A*, *27*, 467–473, 1993.

Tang, I. N., and H. R. Munkelwitz, Aerosol phase transformation and growth in the atmosphere, *J. Appl. Meteorol.*, *33*, 791–796, 1994.

Tang, I. N., K. H. Fung, D. G. Imre, and H. R. Munkelwitz, Phase transformation and metastability of hygroscopic microparticles, *Aerosol Sci. Technol.*, *23*, 443–453, 1995.

Unruh, H.-G., The spontaneous polarization of $(NH_4)_2SO_4$, *Solid State Commun.*, *8*, 1951–1954, 1970.

Weis, D. D., and G. E. Ewing, Infrared spectroscopic signatures of $(NH_4)_2SO_4$ aerosols, *J. Geophys. Res.*, *101*, 18,709–18,720, 1996.

Xu, J., D. Imre, R. McGraw, and I. Tang, Ammonium sulfate: Equilibrium and metastability phase diagrams from 40 to −50°C, *J. Phys. Chem. B*, *102*, 7462–7469, 1998.

T. J. Fortin, J. E. Shilling, and M. A. Tolbert, Department of Chemistry and Biochemistry and Cooperative Institute for Research in Environmental Sciences, University of Colorado, Boulder, CO 80309-0216, USA. (fortint@ucsu.colorado.edu)